



Seismic Capacity Comparisons of Reinforced Concrete Buildings Between Standard and Substandard Detailing

Jirawat Junruang^a, and Virote Boonyapinyo^{a*}

^a Department of Civil Engineering Faculty of Engineering, Thammasat University, THAILAND

ARTICLE INFO

Article history:
Received 24 February 2014
Received in revised form
04 June 2014
Accepted 20 June 2014
Available online
24 June 2014

Keywords:

Seismic Capacity;
Reinforced Concrete
Buildings;
Incremental Dynamic
Analysis;
Seismic Detailing;
SAP 2000.

ABSTRACT

Earthquakes are cause of serious damage through the building. Therefore, moment resistant frame buildings are widely used as lateral resisting system. Generally three types of moment resisting frames are designed namely Special ductile frames (SDF), Intermediate ductile frames (IDF) and Gravity load designed (GLD) frames, each of which has a certain level of ductility. Comparative studies on the seismic performance of three different ductility of building are performed in this study. The analytical models are considered about failure mode of column (i.e. shear failure, flexural to shear failure and flexural failure); beam-column joint connection, infill wall and flexural foundation. Concepts of incremental dynamic analysis are practiced to assess the required data for performance based evaluations. This study found that the lateral load capacity of GLD, IDF, and SDF building was 19.25, 27.87, and 25.92 %W respectively. The average response spectrum at the collapse state for GLD, IDF, and SDF are 0.75 g, 1.19 g, and 1.33 g, respectively. The results show that SDF is more ductile than IDF and the initial strength of SDF is close to IDF. The results indicate that all of frames are able to resistant a design earthquake.

© 2014 Am. Trans. Eng. Appl. Sci.

1. Introduction

Many building in the Thailand are inadequate for seismic loads and could be seriously damaged or could suffer collapse in an earthquake. Hence, the new standard for the building

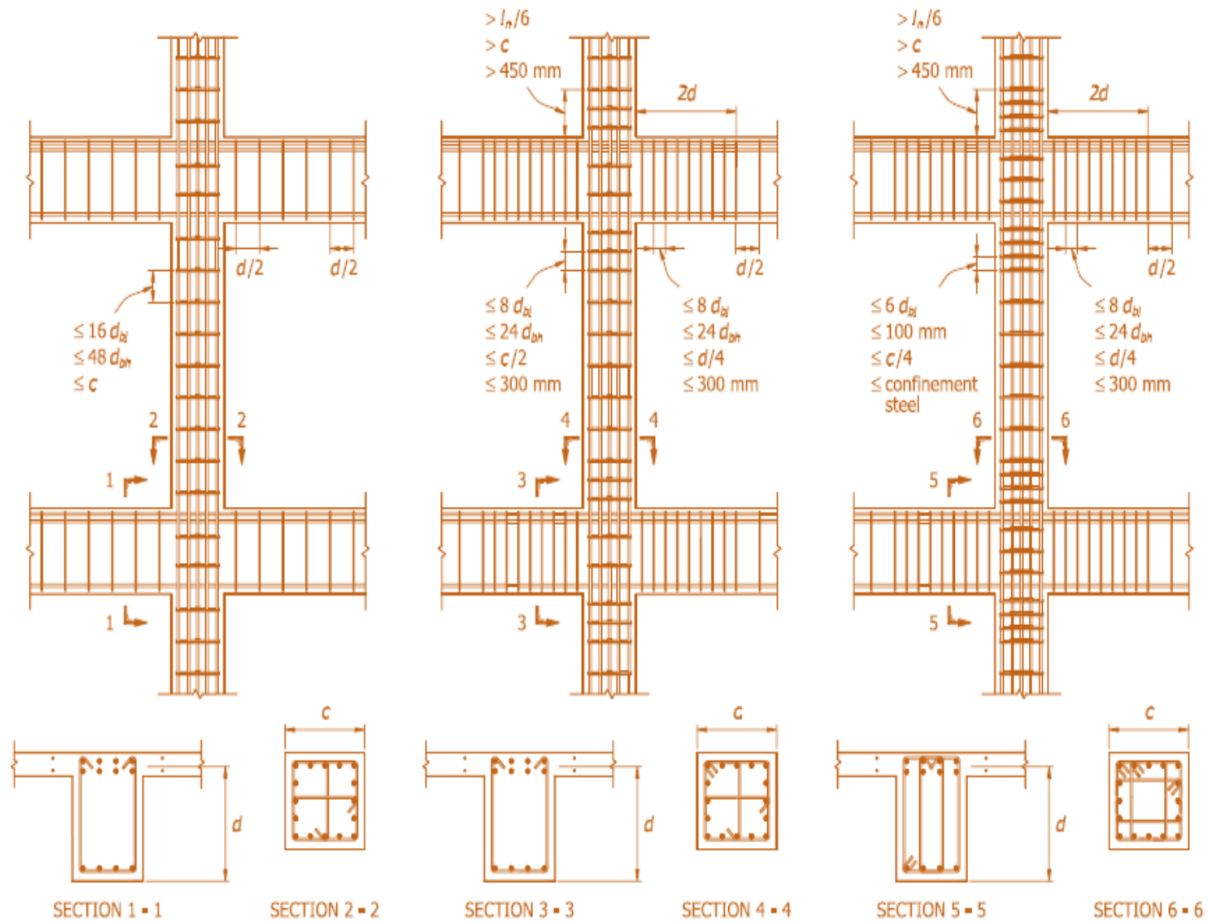
*Corresponding author (Virote Boonyapinyo). Tel/Fax: +66-2-5643001-9 Ext. 3111. E-mail address: bvirote@engr.tu.ac.th. © 2014. American Transactions on Engineering & Applied Sciences. Volume 3 No.3 ISSN 2229-1652 eISSN 2229-1660 Online Available at <http://TuEngr.com/ATEAS/V03/0189.pdf>.

design under seismic loading in Thailand DPT 1302-52 (2009) define three types of moment frames systems namely ordinary moment frames, intermediate ductile frames and special ductile frames (OMF, IDF and SDF) used as lateral resisting system. This study evaluates and compares the performance of three moment resisting frames namely, SDF, IDF and GLD, which three building are designed according to the Thailand DPT 1302-52 (2009) and detailing by the provisions of UBC (1997) and of DPT standard 1301-50 (2007). A computer program SAP2000 (2000) is employed as a means of analysis.

Many researches have investigated the performance and response of structure under earthquake excitation. As a consequence, several researchers and designers are interested in nonlinear static analysis (pushover) and nonlinear dynamic analysis (NTHA). The later method, the convention has been to run one to several different records, each once, producing one to several ‘single-point’ analyses, mostly used for checking the designed structure. Vamvastikos and Cornell (2002) proposed method called ‘incremental dynamic analyses’. Concept of Incremental Dynamic Analysis (IDA) is run nonlinear time history analyses (NTHA) of structure under monotonically scaling up considered ground motion until the response of structure shown collapse. The monotonic scalable ground motion intensity measure (IM) was plotted together with a damage measure (DM) called incremental dynamic analysis curve (IDA curve). The IDA curve contains the necessary information to assess the performance levels or limit-states of the structures.

Since, incremental dynamic analysis required a lot of resources and time-consuming. To reduce analysis times of the convention NTHA, Vamvastsikos and Cornell (2005) propose another method that describes a non-linear static (pushover) combined with NTHA of equivalent single degree of freedom (ESDOF). FEMA P440A (2009) investigates the effect of stiffness and strength degradation on the seismic response of the structures by using concept of ESDOF.

However, all these procedures require accuracy of nonlinear force–deformation curves. In order to capture structural member behavior in non-linear elastic, the model which considers a shear force, a bending moment, and an axial force should be studied. The research related to the model was suggested in the previous works (Sung et al., 2005, 2013; Sharma et al., 2013).



(a) Ordinary Moment Frames (b) Intermediate Ductile Frames (c) Special Ductile Frames

Figure 1: Detailing of reinforced concrete frame.

2. Case study for 5 story reinforced concrete building

Based on the strong column-weak beam design concept, plastic hinges (PHs) should be employed on beam elements in order to dissipate the energy generated by earthquakes. By properly specifying capacity and ductility, sufficient shear strength can be provided by Beam-column joints (BCJs) to allow the development of PHs on beam elements. The strength ratio between beams and columns in the ACI 318-11(2011) code is given as:

$$\sum M_{nc} \geq (6/5)\sum M_{nb} \quad (1)$$

Where $\sum M_{nc}$ is the total nominal flexural strength and also the minimum flexural strength considering the axial and lateral forces of columns connected to a joint; and $\sum M_{nb}$ is the total

*Corresponding author (Virote Boonyapinyo). Tel/Fax: +66-2-5643001-9 Ext. 3111. E-mail address: bvirote@engr.tu.ac.th. © 2014. American Transactions on Engineering & Applied Sciences. Volume 3 No.3 ISSN 2229-1652 eISSN 2229-1660 Online Available at <http://TuEngr.com/ATEAS/V03/0189.pdf>.

nominal flexural strength of beams connected to the joint considering the floor reinforcement (ACI Committee 318, 2011).

The shear capacity of a joint is calculated by considering the repetitive loading on BCJs under earthquakes and energy dissipated by the PHs on beams near the joint, and the induced shear force $V_{jh,u}$ is set as the design shear-force of the joint V_u . The induced shear force is expressed as

$$V_{jh,u} = (A_s + A'_s)\alpha f_y - V_{col} \quad (2)$$

Where A_s and A'_s are the upper and lower rebar areas of the beam, respectively, αf_y is the over strength of the beam rebar, and V_{col} is the shear-force of the column. The A'_s term can be neglected if the rebar is anchored inside the joint. Detailing about reinforced concrete with various ductility (see Figure 1)

2.1 Geometry

Figure 2 and 3 shows the geometry of 5-storey dormitory building used for study. The selected buildings are beam-column reinforced concrete frame without shear wall. The rectangular plan of building measures 14.40×32.00 m. Each story height is 2.80 m. with a total height 14.00 m. The structural system is essentially symmetrical.

Table 1: Cross-section summaries designed for gravity load design columns and beams.

Storey	Description	Dimension	Reinforcement	Stirrup
1-2	C1	0.4×0.3 m.	10-db20 mm.	Rb6 mm.@20cm.
3-5	C2	0.4×0.25 m.	8-db16 mm.	Rb6 mm.@20cm.
1-4	B1	0.25×0.45 m.	6-db16 mm. (T) 6-db16 mm. (B)	Rb6 mm.@20cm.
1-4	B4	0.25×0.45 m.	4-db16 mm. (T) 4-db16 mm. (B)	Rb6 mm.@20cm.
Roof	B8	0.25×0.45 m.	3-db16 mm. (T) 3-db16 mm. (B)	Rb6 mm.@20cm.

All frames were designed with ductility to 8 and 5 in order to examine the influence of the design ductility classes as moment resisting frames with SDF and IDF respectively. For the GLD frame, the structure was designed according to ACI 318-11 (2011). Each pile is of I-shaped 0.40 m. in size and 21m. in length. It is designed for a vertical safe load of 40 tons, the dimension of beam and column (see in Table 1, 2 and 3)

Table 2: Cross-section summaries designed for immediate ductile columns and beams.

Storey	Description	Dimension	Reinforcement	Stirrup
1-5	C	0.4×0.4 m.	12-db20 mm.	3Rb9 mm.@15cm. (H1) 3Rb9 mm.@20cm. (H2)
1-4	B1	0.25×0.5 m.	5-db20 mm. (T) 5-db20 mm. (B)	Rb9 mm.@10cm. (L1) Rb9 mm.@15cm. (L2)
1-4	B4	0.25×0.5 m.	4-db16 mm. (T) 4-db16 mm. (B)	Rb9 mm.@10cm. (L1) Rb9 mm.@15cm. (L2)
Roof	B8	0.25×0.5 m.	3-db16 mm. (T) 3-db16 mm. (B)	Rb9 mm.@10cm. (L1) Rb9 mm.@15cm. (L2)

Table 3: Cross-section summaries designed for special ductile columns and beams.

Storey	Description	Dimension	Reinforcement	Stirrup
1-5	C	0.4×0.4 m.	12-db20 mm.	3Rb9 mm.@15cm. (H1) 3Rb9 mm.@20cm. (H2)
1-4	B1	0.25×0.5 m.	4-db20 mm. (T) 4-db20 mm. (B)	Rb9 mm.@10cm. (L1) Rb9 mm.@15cm. (L2)
1-4	B4	0.25×0.5 m.	4-db16 mm. (T) 4-db16 mm. (B)	Rb9 mm.@10cm. (L1) Rb9 mm.@15cm. (L2)
Roof	B8	0.25×0.5 m.	3-db16 mm. (T) 3-db16 mm. (B)	Rb9 mm.@10cm. (L1) Rb9 mm.@15cm. (L2)

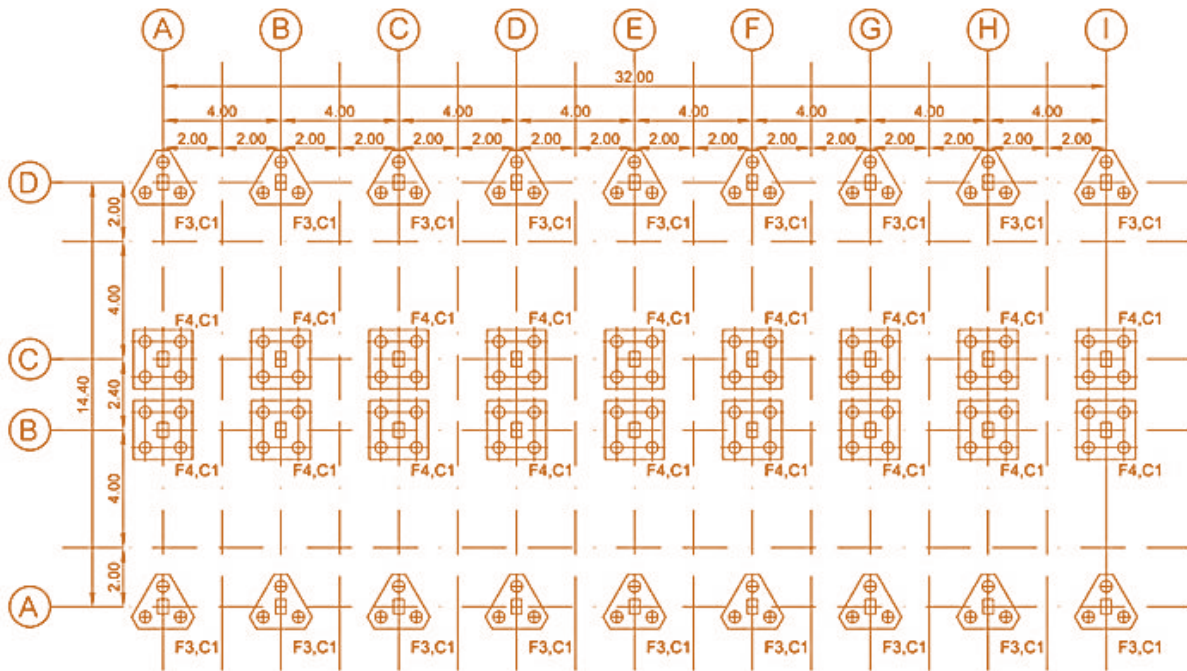


Figure 2: Foundation plans view.

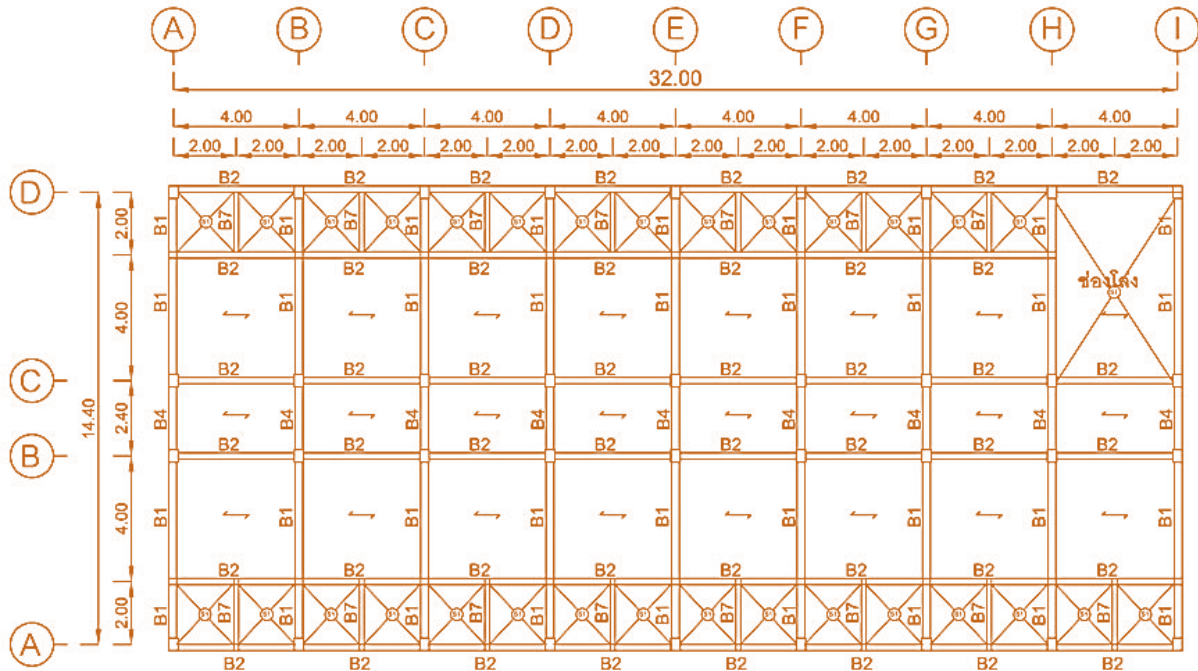


Figure 3: Plan view of buildings.

2.2 Material Properties

In the design, the cylinder compressive strengths of concrete columns and beams are 240 ksc. The yield strengths of steel deformed and rounded bars are 4,000 ksc. (SD 40) and 2400 ksc. (SR 24), respectively. For seismic evaluation, the actual yield strength of steel reinforcement of 4,600 ksc. (SD 40) and 3,480 ksc. (SR 24) are used for SD 40 and SR 24, respectively (Kiattivisanchai, 2001).

3. Analytical modeling

3.1 Plastic hinge setting of beam and columns

The Plastic hinges (PHs) settings of the beams and columns of the frame were established using the method developed by Sung *et al.*, (2005). For a specific RC component, the relationship between the moment and curvature ($M-\phi$), can be established when considering the flexural capacity of the component, as shown in Figure 4 Note that the condition where the shear capacity of the RC component decreases as inelastic deformation proceeds is also included in this approach. As a result, the shear capacity, which consists of the relationship between the transformed moment M_v and rotation θ , as shown in Figure 4(b), can be obtained. By superimposing the diagrams of ($M_b - \theta$) and ($M_v - \theta$), three different types of failure modes (shear failure, flexure to shear failure, and flexure failure) can be illustrated. The PH

characteristics indicated by points A through E in Figure 4, expressed by the relationship between moment and flexural rotation, are therefore definable.

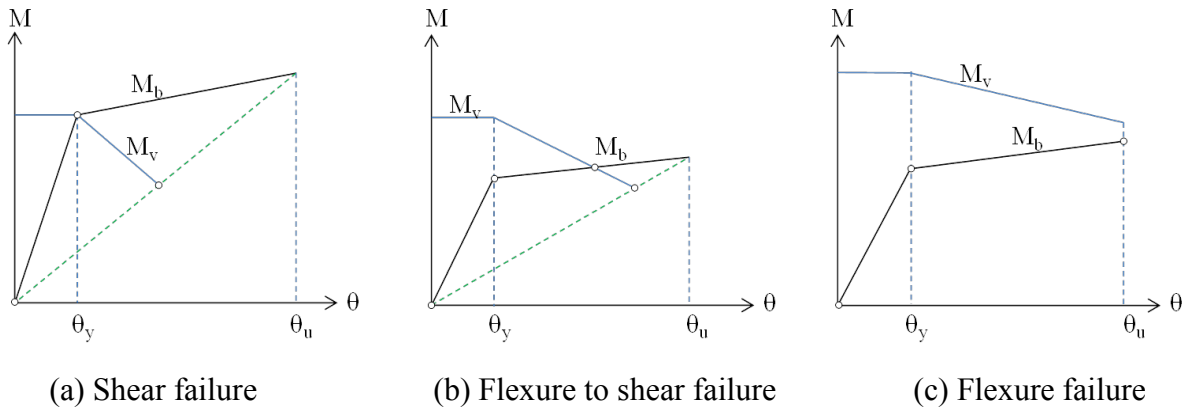


Figure 4: Failure modes of a column or beam and their PH characteristics

3.2 Plastic hinge settings for beam-column-joints

The PH characteristic of BCJs were established using the method developed by Sung *et al.*, (2013), according to FEMA-356 (2000), the nominal shear strength of BCJs can be calculated as

$$V_n = \lambda \gamma \sqrt{f'_c} A_j \quad (3)$$

Where λ is the coefficient of the concrete, and is set as 1 for regular concrete and 0.75 for lightweight concrete; γ is a constant depending on the volumetric ratio of the horizontal confinement reinforcement in the joint and the classification of the BCJ. Specific values of γ can be found in Table 4, where f'_c is the strength of concrete and A_j is the effective cross sectional area of the joint.

Table 4: Values of the constant γ specified in (FEMA 356, 2000)

ρ'	Value of γ				
	Interior Joint with Transverse Beam	Interior Joint without Transverse Beam	Exterior Joint with Transverse Beam	Exterior Joint without Transverse Beam	Knee Joint
<0.003	12	10	8	6	4
>0.003	20	15	15	12	8

* ρ' = volumetric ratio of the horizontal confinement reinforcement in joint.

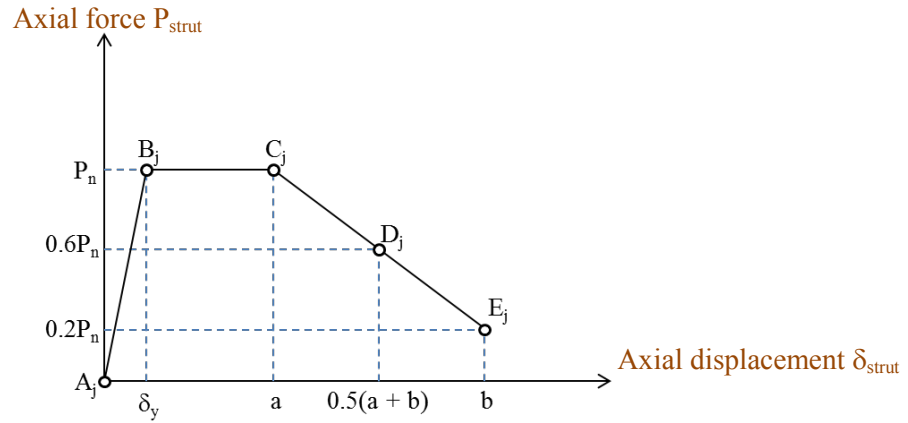


Figure 5: behavior of the PH of a BCJ (Sung *et al.*, 2013).

Based on FEMA-356 (2000), the values used to define the PH characteristics of BCJs are calculated as shown in Figure 5, where A_j is the initial point and B_j represents the yielding. By assuming that the beam-column joints are part of the column and beam hence, the initial stiffness of the PH between A_j and B_j equal to $0.4 E_c A_g$. Since, shear failure is a common cause of failure of a BCJs, the strength at point C_j , the final point of the nonlinear stage, is conservatively set as the same value as at B_j . Point D_j is defined to represent the residual strength, and the strength and axial displacement can be estimated as the mean values at points C_j and E_j , where the strength at E_j is $0.2 P_n$. The BCJ is simulated by using a pair of cross struts in the diagonal direction when resisting horizontal loading, as illustrated in Figure 6. The adjacent components of the BCJ are simulated by a rigid bar with a hinge connection on the end point, where the height of the model is the depth of the beam, and the width equals the effective width of the column. The complex behavior of the BCJ is subsequently simulated by a cross-strut model with an equivalent two-force component. The relationship between the horizontal shear force V and displacement δ is transformed into the direction of the strut, and is derived as

$$P_{strut} = V / 2 \cos \theta \quad (4)$$

$$\delta_{strut} = \delta \times \cos \theta \quad (5)$$

Where P_{strut} is the equivalent axial force on the strut; V is the equivalent horizontal shear force on the strut; δ_{strut} is the equivalent axial displacement; δ is the equivalent horizontal displacement; and θ is the angle of the strut from horizontal.

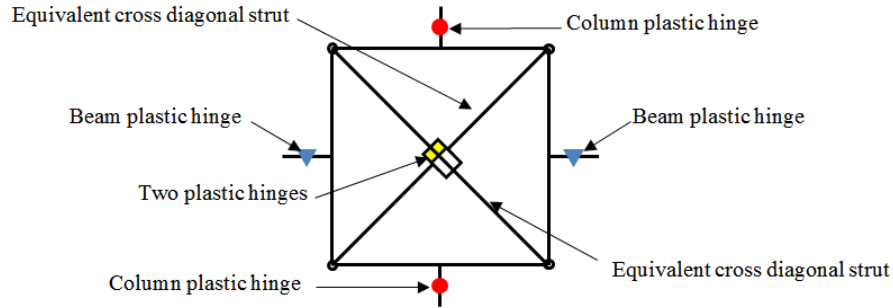


Figure 6: Cross-strut model for BCJ simulation.

3.3 Masonry infill wall

As mentioned earlier, equivalent strut concept will be used to model masonry infill wall. Based on this concept, the stiffness contribution of infill wall is represented by an equivalent diagonal compression strut as shown in Figure 7. Thickness and modulus of elasticity of strut are assumed to be the same as those of infill wall. Moreover, width of equivalent strut a , is determined, which was suggested by FEMA-273 (1997).

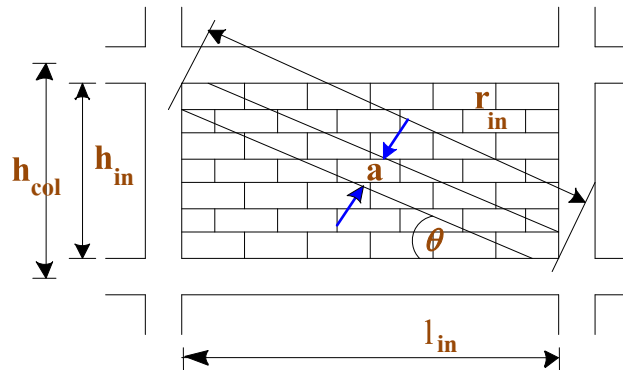


Figure 7: Equivalent diagonal compression strut model (FEMA-273, 1997).

$$a = 0.175(\lambda_1 h_{col})^{0.4} r_{in} \quad (6)$$

$$\lambda_1 = \left[\frac{E_{me} t_{in} \sin 2\theta}{4E_{fe} I_{col} h_{in}} \right]^{\frac{1}{4}} \quad (7)$$

Where E_{me} is modulus of elasticity of masonry infill wall, E_{fe} is modulus of elasticity of frame material, I_{col} is moment of inertia of column section, t_{in} is thickness of infill panel. In

SAP 2000, equivalent diagonal compression strut will be modeled as an axial element having a nonlinear axial hinge along its length. According to FEMA-273 (1997), idealized force-displacement relations for infill wall are defined by a series of straight-line segment. In order to determine the expected strength of strut, R_s the expected infill shear strength, V_{ine} , is used. Therefore, the axial compression strength of equivalent strut R_s can be obtained by solving equation as shown.

$$V_{ine} = \tau_0 l_{in} t_{in} + \mu_f R_s \sin \theta \quad (8)$$

Where τ_0 is an average value of cohesive strength, μ_f is a typical value for the coefficient of friction, l_{in} is length of infill panel and t_{in} is thickness of infill panel. These recommended values are used in the calculation of shear strength of masonry infill walls in this study.

$$V_{ine} = R_s \cos \theta = (l_{in} / r_{in}) R_s \quad (9)$$

$$R_s = \frac{\tau_0}{1 - \mu_f (h_{in} / l_{in})} r_{in} t_{in} \quad (10),$$

Where r_{in} is length of diagonal of infill panel, h_{in} is height of infill panel

4. Artificial Ground Motions

To evaluate the seismic performance of the reinforced concrete structure by incremental dynamic analysis (IDA), Vamvatsikos and Cornell (2005) suggests that the response of the 20 ground motion should be used for evaluating performance of reinforced concrete building. The ground motions in this study were generated corresponding to design spectrum of Bangkok Thailand (Zone5) (DPT 1302-52, 2009) (*see* in Figure 7).

5. Nonlinear static pushover

Generally, in pushover method the structure is loaded with “lateral load pattern” and is pushed statically to “target displacement”. The lateral load might be considered as “force” or “displacement”. The loading is monotonic with the effects of the cyclic behavior and load reversals and with damping approximations.

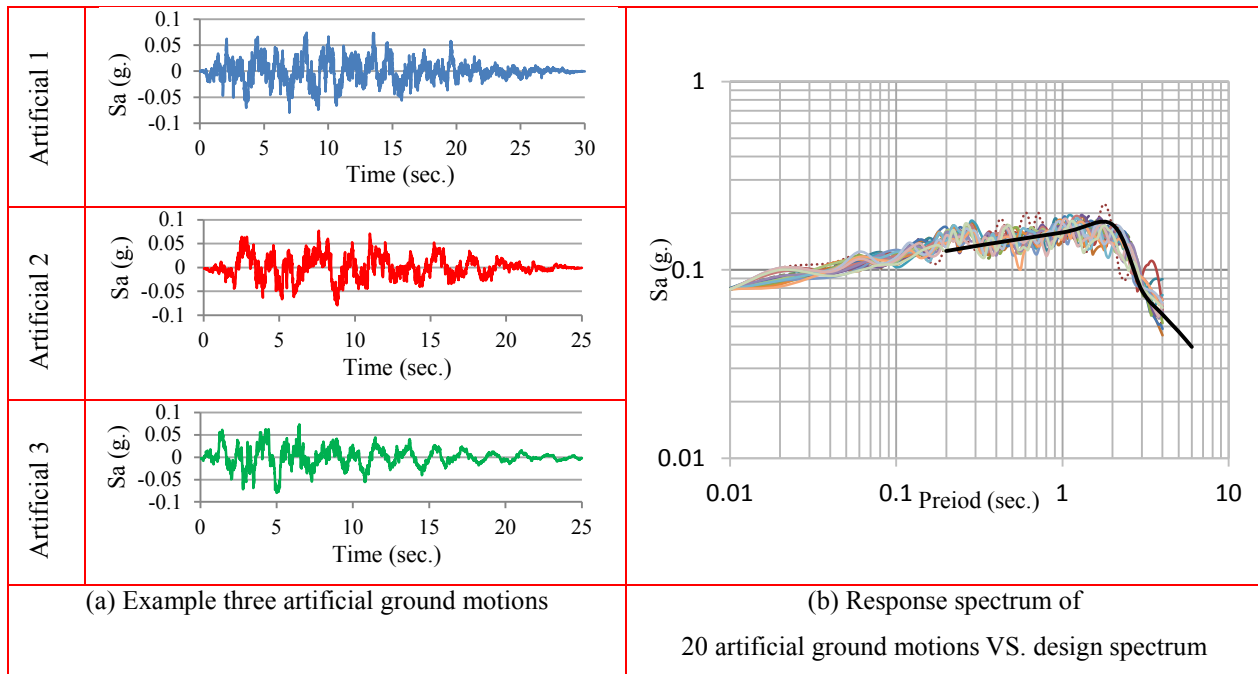


Figure 7: Artificial ground motions generated corresponding with the design spectrum for the inner area of Bangkok

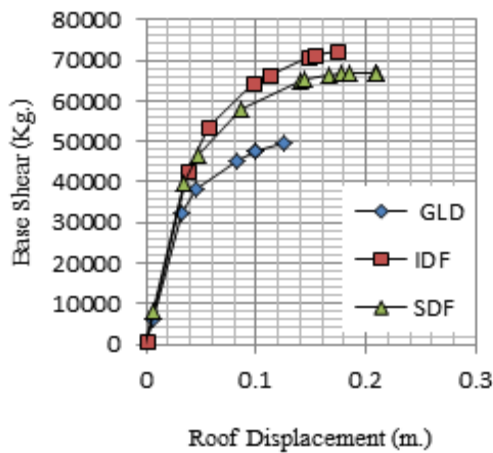


Figure 8: Base shear vs. maximum roof displacement of 5-storey dormitory building.

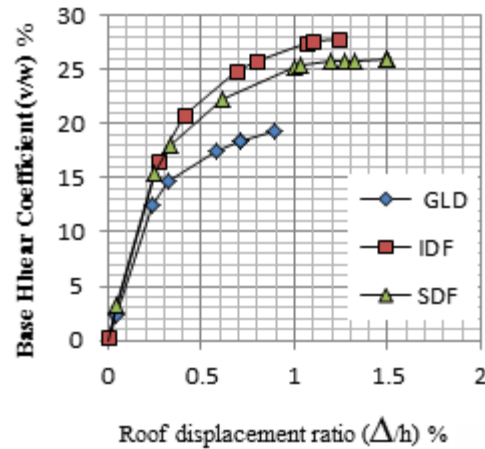


Figure 9: Base shear coefficients vs. roof drift ratio of 5-storey dormitory building.

The static pushover analysis is performed on each model to evaluate the lateral strength and post-yield behavior. Base shear vs. maximum roof displacement pushover for 5 storey buildings are shown in Figure 8. For one bay framed, displacement-control loading is applied to the models using a load pattern based on fundamental period of the structures to account for inherent response of the buildings to lateral loadings. As it is shown in Figure 8, the stiffness of SDF is closed to IDF whereas; the ductility of SDF is much greater resulting in the superiority of SDF in input

*Corresponding author (Virote Boonyapinyo). Tel/Fax: +66-2-5643001-9 Ext. 3111. E-mail address: virote@engr.tu.ac.th. © 2014. American Transactions on Engineering & Applied Sciences. Volume 3 No.3 ISSN 2229-1652 eISSN 2229-1660 Online Available at <http://TuEngr.com/ATEAS/V03/0189.pdf>.

energy absorption. The considerable drop in load carrying capacity of the buildings is due to limit rotations assigned to beam column connections to account for design provisions and considerations which high lights the fact that SDF connections shall be designed such that more deformability is obtained. Moreover, base shear coefficients vs. roof drift ratio pushovers for 5 storey buildings are shown in Figure 9.

From the pushover curve in Figure 9, the results of lateral resistance of three building are hereinafter. The 1st stage, the relationship between base shear and lateral roof displacement represent a linear relationship. Until continue loading of lateral force over elastic period result in the yielding of B4 (short beam) and the rupture of brick wall. These phenomena led to a few reduction of lateral force resistance. The most reduction of lateral force resistance can be observed when the failures of B1 beam (long beam) occurred. All of the failure of B1 beam appears at the right side tail because of the vertical force from self-weight load and live load. The vertical force cause the negative moment at bilateral tails while the lateral force cause the positive moment in B1 beam at position near the lateral force at the left side. The lateral force induces the destructive of the moment at the left side tail. Moreover, the negative moment at the right side tail of B1 beam can be generated, result in the supplement of negative moment at the tail. Since the positive and negative moment resistances B1 beam were equal, negative moment at right side tail can reach the maximum moment resistance and failure first. The loss of vertical and lateral resistance force of the structure at failure condition can be occurred when there are a great damage in the joint until the stability of the building gets lost. Based on the strong column weak beam concept design, there are a little damage in the column. Displacement coefficient between the layers of the building is a variable that can be described how structure behavior responded and where is the most movement between the layers occurred.

The result from nonlinear static pushover analysis in Figure 9 also shown that the most inter-storey drift can be observed at the second floor, the lateral load capacity of GLD, IDF, and SDF building was 19.25, 27.87, and 25.92 %W (W = total building weight), respectively, and roof displacement was 0.89, 1.24, and 1.49 %H (H = total building height), respectively.

6. Incremental Dynamic Analysis

Incremental Dynamic Analysis (IDA) of multi degree of freedom (MDOF) has been reported by Vamvatsikos and Cornell (2002) involves performing a series of nonlinear dynamic analyses of

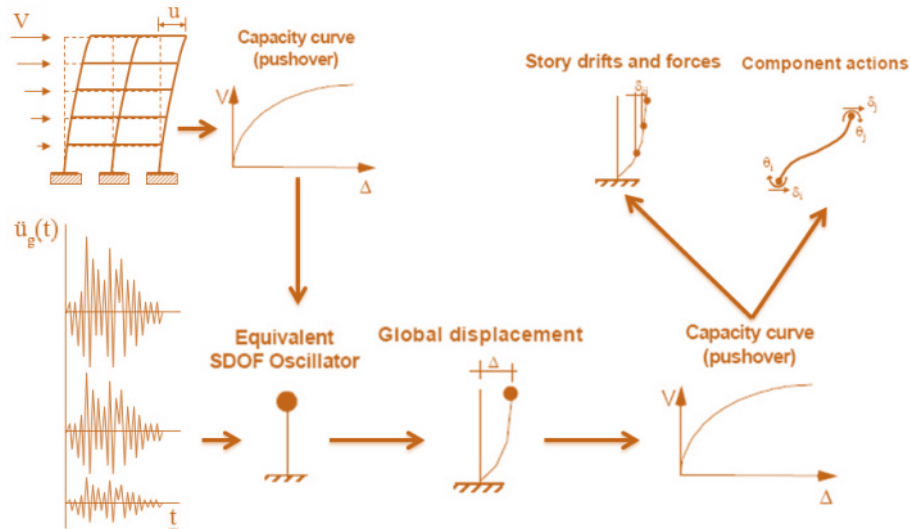
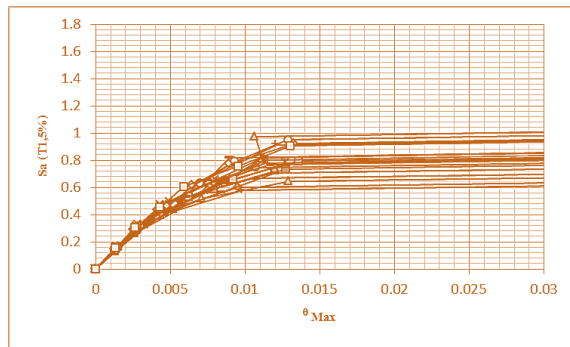
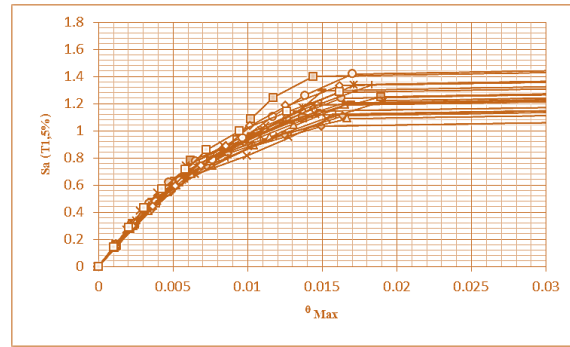


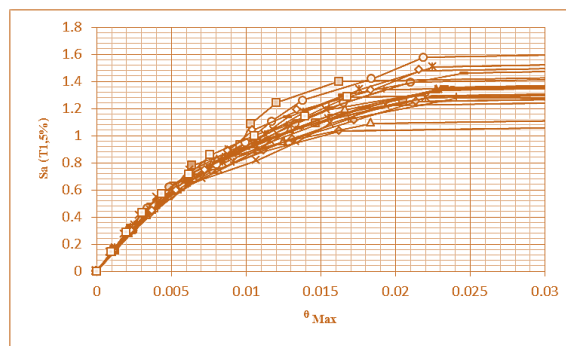
Figure 10: Concept of incremental dynamic analysis of equivalent single degree of freedom



(a) Gravity load designed.



(b) Intermediate designed frame



(c) Special designed frame.

Figure 11: All twenty IDA curves for 5-storey buildings.

a structural model for multiple records by scaling each record to several levels of intensity that are suitably selected to uncover the full range of the model's behavior: from elastic to yielding and nonlinear inelastic, finally leading to global dynamic instability. Each dynamic analysis can be characterized by at least two scalars, an intensity measure (IM), which represents the scaling

*Corresponding author (Virote Boonyapinyo). Tel/Fax: +66-2-5643001-9 Ext. 3111. E-mail address: bvirote@engr.tu.ac.th. © 2014. American Transactions on Engineering & Applied Sciences. Volume 3 No.3 ISSN 2229-1652 eISSN 2229-1660 Online Available at <http://TuEngr.com/ATEAS/V03/0189.pdf>.

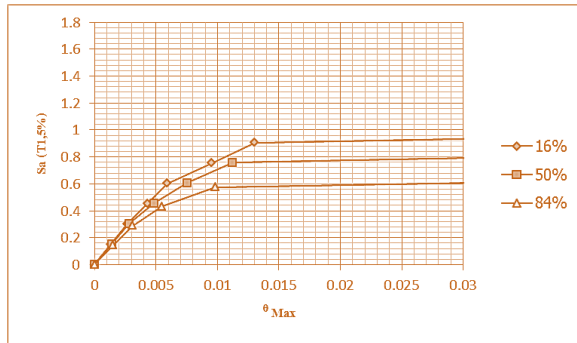
factor of the record [e.g., the 5% damped first-mode spectral acceleration $Sa(T1,5\%)$] and an engineering demand parameter (EDP), which monitors the structural response of the model [e.g., peak inter-story drift ratio θ_{max}].

The concept of combining between nonlinear static and nonlinear dynamic (time history) analysis (NTHA) has been suggested by Vamvatsikos (2005). The pushover curves from nonlinear static are represent the lateral behavior of whole structure, and then defined it into the single degree of freedom to be equivalent of MDOF structure. Concepts of IDA by ESDOF (see in Figure 10), and the result of IDA by ESDOF of 5-storey dormitory building with various ductility are show in Figure 11.

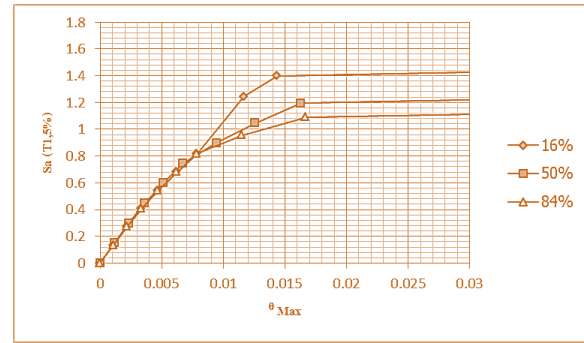
The results from Incremental dynamic analysis of equivalent single degree of freedom are shown in Figure 11. It can be interpret as follow: at the beginning, the linearity was controlled by initial stiffness, so no distributions of the data until the earthquake violence reach up to the yield point. In this stage, some beams are reaching yield point so slope of IDA decrease. Then, the strength of the structure was improved until reach the maximum pushover curve. At this point, IDA slope was going to flat line which was implying that the structure was dynamic instability.

Figure 11 shows the IDA curves display a wide range distribution of data, thus, it is essential to summarize randomness of data and quantify introduced by the records. The central value (e.g., the median) was used for easy interpretation of data. Consequently, it has been chosen to calculate the 16%, 50% and 84% fractile values of DM and IM capacity for each limit-state. For example, summarized capacities for each limit-state for 5-storey buildings are shown in Figure 12. Dynamic characteristics of these aforementioned buildings could be readily observed through the use of median IDA curves. As it is seen, linear slope is increased as behavior factor is decreased through the models. That is, IDF is the laterally stiffest since its members are designed stronger in comparison with other types of building. However, special consideration and provisions imposed for SDFs dedicate superior deformability which can be clearly implied by IDA. One can investigate better performance of SDF through comparing different Sa evaluation and corresponding demand, reported by the structural model.

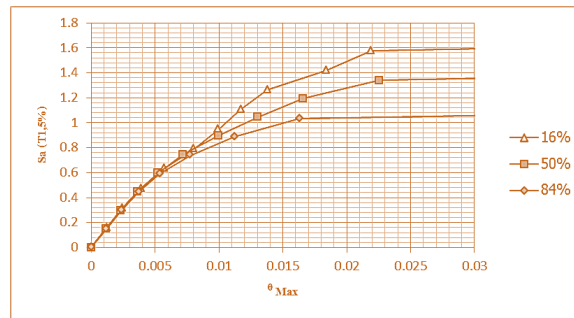
Other information may be extracted from IDA curves to pronounce the suitability and capability of moment frames as show in Table 5 and Table 6 for yield state and collapse state, respectively.



(a) Gravity load designed.



(b) Intermediate designed frame



(c) Special designed frame.

Figure 12: The summary of the IDA curves into their 16%, 50% and 84% fractile curves for 5-storey buildings.

Table 5: Yield state from IDA curves of buildings.

	Period of building (sec)	Sa (T1, 5%) (g)	θ Max (%)	Roof displacement (m.)	Base shear (kg.)
GLD	0.719	0.31	0.29	0.032	32,188.21
IDF	0.653	0.448	0.366	0.038	42,795.52
SDF	0.653	0.409	0.328	0.034	39,923.79

Table 6: Collapse state from IDA curves of buildings.

	Period of building (sec)	Sa (T1, 5%) (g)	θ Max (%)	Roof displacement (m.)	Base shear (kg.)
GLD	0.719	0.75	1.12	0.105	47,723.00
IDF	0.653	1.19	1.62	0.147	70,981.41
SDF	0.653	1.33	2.25	0.195	66,978.47

In the past, conventional model used to perform pushover analysis must be set the failure criteria by assuming to have collapsed if the Maximum inter story drift ratio exceed of 3%, 2.5%, 2%, and 1% for SDF, IDF, ODF, and GLD, respectively. In this study, the analytical models consider all types of failure mode, (i.e. flexural failure, shear failure, flexural to shear failure,

*Corresponding author (Virote Boonyapinyo). Tel/Fax: +66-2-5643001-9 Ext. 3111. E-mail address: bvirote@engr.tu.ac.th. © 2014. American Transactions on Engineering & Applied Sciences. Volume 3 No.3 ISSN 2229-1652 eISSN 2229-1660 Online Available at <http://TuEngr.com/ATEAS/V03/0189.pdf>.

beam-column joint connection failure, infill wall failure and flexural foundation failure). Thus, pushover curve consider the failure criteria automatically. Accuracy of pushover curves is significant because it's able to absorb and dissipate the earthquake energy. If areas of pushover curves extend too much, they are affecting to the seismic capacity of building. The results at collapse state shown that the maximum inter story drift ratio of GLD, IDF, and SDF building in Bangkok was 1.12%, 1.62%, and 2.25% respectively, and can interpret to roof displacement as 0.105m. 0.147m. and 0.195m., respectively. Base shear was 47,723 kg. 70,981kg. and 66,978kg., respectively and response spectra acceleration at fundamental periods with 5% damping was 0.75, 1.19, and 1.33 g, respectively. The results showed that the different detail of building leads to the highly different lateral capacity of the structures.

7. Conclusion

This study involves seismic performance and evaluations of 5-storey dormitory buildings which having different structural detailing (i.e., SDF, IDF and GLD). The analytical models used in this study emphasize on the plastic hinges (PHs) in beams and columns. Three types of PHs were studied include shear failure, flexure to shear failure, and flexure failure. The initial stiffness of PHs in beam-col connection was considered as a part of the column and the PH characteristics of BCJs are calculated according to FEMA-273. Based on this study, seismic performance for all buildings can be explained as follow:

- (1) The analytical model considers all type of failure mode (i.e. flexural failure, shear failure, flexural to shear failure, beam-column joint connection failure, infill wall failure and flexural foundation failure) shows the accuracy pushover curve. As a result, seismic capacities of building by incremental dynamic analysis method are more accuracy than conventional model.
- (2) Using the concept of ESDOF for evaluating the seismic performance of the studied building by the mean of IDA can reduce the computational time from 90 minutes per load case for MDOF to 6 minutes per load case for ESDOF (about 93% of computational time reduced)
- (3) The results also shown that lateral load capacity of GLD, IDF, and SDF building in Bangkok was 19.25, 27.87, and 25.92 %W (W = total building weight), respectively, and roof displacement was 0.89, 1.24, and 1.49 %H (H = total building height), respectively. At collapse state, response spectra acceleration at fundamental periods with 5% damping was 0.75, 1.19, and 1.33 g, respectively. GLD building was designed by considered gravity load

only. Therefore, the detailing of steel was not follow to Thailand seismic code (DPT 1302-52, 2009). Consequence, seismic capacity of the building has shown the lowest value.

- (4) The seismic performance of IDF and SDF building from initial to yield stage were almost the same. Because of the higher lateral load design for IDF, IDF building results in higher base shear capacity than SDF building.
- (5) As far as the effect of the ductility class is concerned, frames of SDF, IDF, and GLD ductility classes are to perform satisfactorily during a design earthquake. Although SDF was designed for five-eighths value of the designed lateral load of IDF, all components of SDF had to satisfy the applicable special proportioning and detailing requirement to have a level of adequate toughness enabling the structure to perform well during a design earthquake. It demonstrated the successful application of the strong-column–weak-beam implemented in the capacity design.

8. Acknowledgements

This work was supported by the National Research University Project of Thailand Office of Higher Education Commission. The valuable comments of the anonymous reviewers of the paper are also acknowledged.

9. References

- ACI (2011). Building code requirements for structural concrete and commentary. *Report No. ACI 318-11*, Farmington Hills, Michigan, U.S.A., American concrete Institute.
- DPT (2007). Additional standard for building designed under seismic load. *Report No. DPT 1301-50*, Department of Public Works and Town and Country Planning (in Thai).
- DPT (2009). Standard for building designed under seismic load. *Report No. DPT 1302-52*, Department of Public works and town and country planning (in Thai).
- FEMA (1997). Guidelines for the seismic rehabilitation of building. *Report No. FEMA-273*, NEHRP Commentary on the guidelines for the seismic rehabilitation of building. *Report No. FEMA-274*, Federal emergency management agency. Washington D.C.
- FEMA (2000). Pre-standard and commentary for the seismic rehabilitation of buildings. *Report No. FEMA-356*, Building seismic safety council, Washington D.C.
- FEMA (2009). Effects of strength and stiffness degradation on seismic response. *Report No. FEMA-P440A*, Federal emergency management agency, Department of homeland security (DHS).

*Corresponding author (Virote Boonyapinyo). Tel/Fax: +66-2-5643001-9 Ext. 3111. E-mail address: virote@engr.tu.ac.th. ©2014. American Transactions on Engineering & Applied Sciences. Volume 3 No.3 ISSN 2229-1652 eISSN 2229-1660 Online Available at <http://TuEngr.com/ATEAS/V03/0189.pdf>.

- Kiattivisanchai, S. (2001). Evaluation of seismic performance of an existing medium-rise reinforced concrete frame building in Bangkok, M.Eng thesis, Thesis No. ST-01-11, Asian Institute of technology
- SAP 2000 (2000). Integrated finite element analysis and design of structure: Analysis reference, *Computers and Structures, Inc.*, Berkeley, California.
- Sharma AK., G.R. Reddy, K.K. Vaze, R. Eligehausen. (2013). Pushover experiment and analysis of a full scale non-seismically detailed RC structure. *Engineering Structures*, Vol.46
- Sung Y.C., Liu KY, Su CK, Tsai IC and Chang KC. (2005). A study on pushover analyses of reinforced concrete columns. *Journal of Structural Engineering and Mechanics*, 21(1): 35–52.
- Sung Y.C., T.K. Lin, C.C. Hsiao, and M.C. Lai. (2013). Pushover analysis of reinforced concrete frames considering shear failure at beam-column joints. *EARTHQUAKE ENGINEERING AND ENGINEERING VIBRATION*, Vol.12, No.3
- Prakit Chomchuen and Virote Boonyapinyo. (2012). Comparisons of current seismic assessment methods for non-Seismic designed reinforced concrete bridges, *15th World Conference on Earthquake Engineering*, 24-28 September, Lisbon, Portugal
- UBC (1997). Uniform building code, structural engineering designed provisions. *Report No. UBC 1997*, International Conference of Building Officials (ICBO).
- Vamvatsikos, D. and Cornell, C. A. (2002a). Incremental dynamic analysis, *Earthquake Engineering and Structural Dynamics*, 31(3): 491–514.
- Vamvatsikos, D. and Cornell, C. A. (2005). Seismic performance, capacity and reliability of structures as seen through incremental dynamic analysis. Department of civil and environmental engineering, Stanford University.
-



Jirawat Junruang is a PhD student in Department of Civil Engineering at Thammasat University, Thailand. He received his B.Eng. from King Mongkut's University of Technology North Bangkok, Thailand. He earned a master degree in Civil Engineering from Thammasat University, in 2013. Jirawat is interested in earthquake-resistant design and evaluation for buildings.



Dr. Virote Boonyapinyo is an Associate Professor of Department of Civil Engineering at Thammasat University, Thailand. He received his B.Eng. and M.Eng. from Chulalongkorn University. He continued his D.Eng. Study at Yokohama National University, Japan, where he obtained his D.Eng. in Civil Engineering. Dr. Virote is interested in wind- and earthquake-resistant design for high-rise buildings and long-span bridges, and steel structures.

Peer Review: This article has been internationally peer-reviewed and accepted for publication according to the guidelines given at the journal's website.